

# Design, Synthesis, Molecular Docking and Crystal Structure Prediction of New Azasugar Analogues of $\alpha$ -Glucosidase Inhibitors

Venerando Pistarà,\*<sup>[a]</sup> Antonio Rescifina,<sup>[a]</sup> Francesco Punzo,<sup>[a]</sup> Graziella Greco,<sup>[a]</sup> Vincenzina Barbera,<sup>[a]</sup> and Antonino Corsaro<sup>[a]</sup>

**Keywords:** Medicinal chemistry / Enzymes / Inhibitors / Carbohydrates / Azasugar mimics / Amination / Reduction / Structure–activity relationships

This work deals with the design and synthesis of  $\alpha$ -glucosidase inhibitors. In order to perform this task, a molecular docking study was carried out with the *N*-terminal catalytic subunit of human maltase glucoamylase, which evidenced a partially empty, hydrophobic part of the docking pocket. As a consequence, we decided to improve the docking abilities of the known  $\alpha$ -glucosidase inhibitor MDL 73495 and carried out the synthesis of new *N*-glycosyl-derived analogues. The addition of a hydrophobic methyl group at C-5'ax, the concomitant elimination of the equatorial hydroxy group, the inversion of the configuration at C-4 in the sugar unit and the

substitution of the hydroxy group at C-6' with an amino group led to 6'-deoxy-6'-amino-6a. This compound showed the lowest in silico binding affinity among a set of compounds, whose experimental activity has been reported. Bearing these results in mind, we synthesized 6a and 6b. Because of the lack of large amounts of products, which are necessary to perform crystallization, the crystal structures of 6a and 6b were predicted in silico. These can be considered as models for future X-ray powder diffraction characterization of these two compounds.

## Introduction

Among carbohydrate-processing enzymes,  $\alpha$ - and  $\beta$ -glucosidases are the most extensively studied.<sup>[1]</sup> This class of enzymes is responsible for the catalytic cleavage of the glycosidic bond, which involves a terminal glucose. In particular,  $\alpha$ -glucosidase has become an attractive target because it catalyzes the final step in the digestive process of carbohydrates by the hydrolysis of a glycosidic bond in oligo- or polysaccharide chains. Indeed, the modification or inhibition of its catalytic activity resulted in the retardation of glucose absorption and decrease in postprandial blood glucose level.<sup>[1]</sup> Therefore, glucosidase inhibitors represent an interesting class of potential drugs for the treatment of diabetes,<sup>[2]</sup> obesity,<sup>[3]</sup> lysosomal storage diseases,<sup>[4]</sup> other carbohydrate-mediated diseases such as cancer,<sup>[5]</sup> viral infections and hepatitis.<sup>[6]</sup>

Due to these biological activities, in recent years synthetic efforts have been directed towards the design,<sup>[7]</sup> synthesis and bioevaluation of new carbohydrate mimics, which are analogues of natural acarbose. This is the first  $\alpha$ -D-glucosidase inhibitor (GI) approved for the treatment of type II diabetes<sup>[2,8]</sup> and contains a carbasugar valienamine moiety, which is essential for its bioactivity.<sup>[9]</sup> Most GIs that

have been reported are structurally related to acarbose (Figure 1). Typical examples are the naturally occurring voglibose<sup>[10]</sup> and other carbohydrate mimics, such as polyhy-

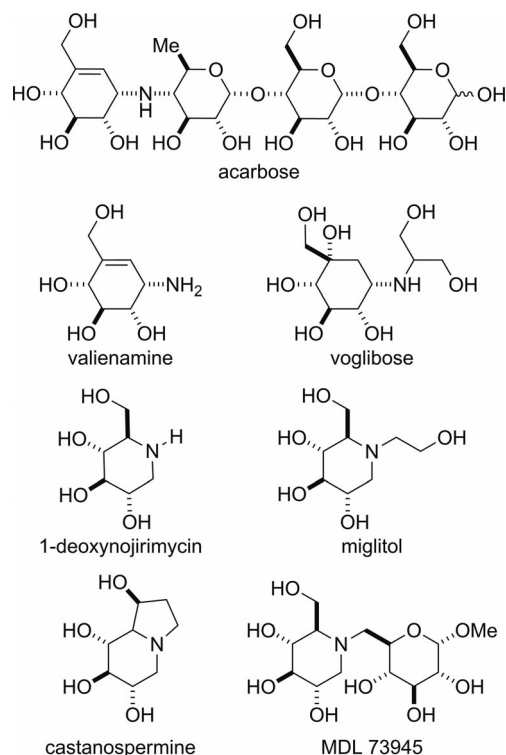


Figure 1. Structural relationships between some GIs.

[a] Dipartimento di Scienze del Farmaco, Università di Catania, Viale A. Doria 6, 95125 Catania, Italy  
Fax: +39-095-580138  
E-mail: vpistara@unict.it

Supporting information for this article is available on the WWW under <http://dx.doi.org/10.1002/ejoc.201100832>.

droxypiperidines (aza- or iminosugars),<sup>[11]</sup> 1-deoxynojirimycin, miglitol and castanospermine,<sup>[11e]</sup> which have been approved as medicines (Figure 1).<sup>[11f]</sup>

The continuing demand for more potent molecules has stimulated the design of pseudodisaccharide derivatives. In addition to these, MDL 73945,<sup>[2a]</sup> a 1-deoxynojirimycin *N*-glycosyl derivative (Figure 1), shows a potent and selective intestinal GI activity and it is a unique example where the amine is linked to C-6 of a 6-deoxy glucoside. To the best of our knowledge, the sole reported synthesis<sup>[12]</sup> of this molecule concerns the condensation reaction between the appropriate hydroxyl-protected 1-deoxynojirimycin derivative with a hydroxyl-protected glycosyl triflate or halide.

Among the synthetic routes to 1-deoxynojirimycin and its derivatives, the double reductive amination of an aldohexos-5-ulose with a primary amine is a useful alternative thanks to the simple preparation of the starting materials.<sup>[13]</sup>

In the frame of our research on the chemical valorization of lactose, in recent years, we have studied the reactivity of the double bond of its 4'-unsaturated derivative towards the addition of the methylene-zinc-iodide complex<sup>[14]</sup> in order to clarify the stereochemical aspect of these reactions and to obtain 1,5-dicarbonyl analogues of *L*-arabino-hept-5-ulose,<sup>[15]</sup> which are valuable intermediates in the preparation of high value-added compounds such as cyclitols (*epi*- and *D*-*chiro*-inositol)<sup>[16]</sup> and azasugars.<sup>[13]</sup>

Here we report the design, which is based on molecular docking studies and inspection of X-ray structures of known GIs in complexes with the *N*-terminal catalytic subunit of human maltase glucoamylase (NtMGAM), and synthesis of a new *N*-glycosyl-derived analogue of MDL 73945, with an *in silico* potency in the order of nM.

Moreover, without reasonable quantities of products to perform crystallizations, we carried out an *in silico* study aimed at the prediction of their crystal structures. These results can be used as models for structural studies based on X-ray powder diffraction (XRPD).

## Results and Discussion

### Design

The rational design of the new  $\alpha$ -GIs started from the inspection of the crystal structure of miglitol in the catalytic site of NtMGAM, recently reported by Pinto and Rose (PDB ID 3L4W).<sup>[17]</sup> Two water molecules, tightly bound by hydrogen bonds to D366, D443, D571 and W539 residues, are present in the catalytic -1 domain, according the nomenclature of Davies et al.,<sup>[18]</sup> with one located inside to the pocket, although W539 is engaged in a hydrogen bond with the 6-OH group of miglitol and interacts with a negatively charged portion of the pocket, which takes up space that could be filled by an opportune substitution on the ligand (Figure 2). Moreover, another portion of the pocket, located down to H-4, remains empty and shows hydrophobic character.

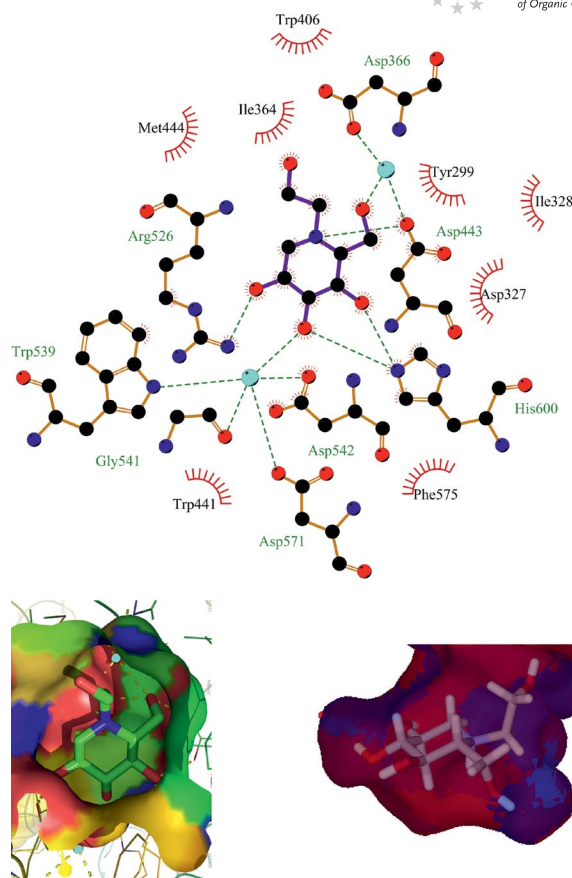


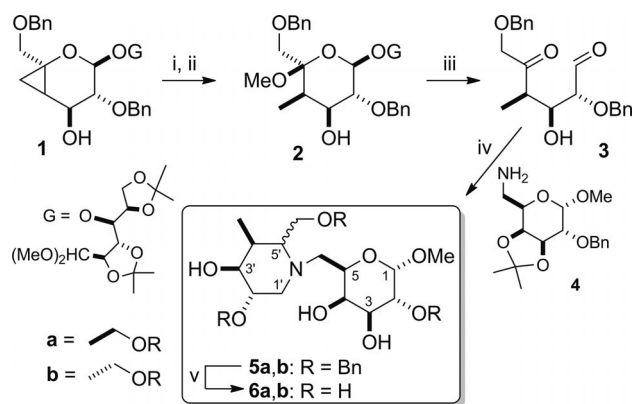
Figure 2. The X-ray structure of miglitol complexed with NtMGAM. 2D schematic view of hydrogen bonds and hydrophobic interactions (top). 3D analogue with the catalytic pocket surface shown as an electrostatic potential surface (bottom left) and the catalytic pocket visualized as a hydrophobic surface (bottom right). In the top and bottom left representations, the two water molecules are depicted in turquoise. The 2D plot was prepared with LigPlot<sup>+</sup>.<sup>[19]</sup>

These observations suggest that it is possible to improve the fit of the ligand by inserting a polar or positively charged group in the equatorial position at C-6 and/or a lipophilic group in the axial position at C-5 of miglitol. With the aim of using lactose as a starting material, we carried out preliminary docking studies with the introduction of modifications to well known  $\alpha$ -GI MDL 73945. The insertion of a hydrophobic methyl group at C-5'<sub>ax</sub>, with the concomitant elimination of the corresponding equatorial hydroxy group, the inversion of the configuration at C-4 in the sugar unit, i.e. the glucose, and the substitution of the hydroxy group at C-6' with an amino group in MDL 73945, gave 6'-deoxy-6'-amino-**6a** as the lead  $\alpha$ -GI with a calculated  $K_i$  value of 686 pM (*vide infra*). However, in this paper, we focus our attention on the synthesis of **6a**.

### Chemistry

Access to the *C*-4-methyl-1,5-dicarbonyl sugar **3** was gained from the electrophilic ring opening of the cyclopropyl adduct **1**, which was obtained in a near quantitative yield and high stereoselectivity from the Simmons–Smith

reaction of hex-4'-eno unsaturated lactose.<sup>[14]</sup> The cyclopropyl adduct **1** was treated with mercuric trifluoroacetate in dry methanol to give, after exchange with NaCl, the corresponding organomercuric chloride in high regio- and stereoselectivity and high yield (Scheme 1).<sup>[20]</sup> The crude reaction mixture was used without purification for reductive demercuration with lithium aluminium hydride to afford, after flash chromatography, 4'-C-deoxy-4'-methyl-1',5'-bisglycoside **2** (78% yield). This was then hydrolyzed by treatment with trifluoroacetic acid to give the C-4-methyl-1,5-dicarbonyl sugar **3**, which exists predominantly in two anomeric  $\alpha$ - and  $\beta$ -oxetanoyl forms (in a 1:1.06 ratio), which are derived from hemiacetalization of the C-3 hydroxy group onto the aldehydic carbonyl group.<sup>[20]</sup>



Scheme 1. i) a)  $\text{Hg}(\text{CF}_3\text{COO})_2$ , MeOH; b) NaCl satd. sol; ii)  $\text{LiAlH}_4$ , tetrahydrofuran; iii)  $\text{CF}_3\text{COOH}$ ,  $\text{CH}_3\text{CN}/\text{H}_2\text{O}$ ; iv)  $\text{NaBH}_3\text{CN}$ ,  $\text{CH}_3\text{COOH}$ , dry MeOH; v)  $\text{H}_2$ , Pd/C, MeOH.

The sugar **3** was treated with  $\text{NaBH}_3\text{CN}$  and methyl 6-amino-6-deoxy-3,4-*O*-isopropylidene- $\alpha$ -D-galactopyranoside (**4**)<sup>[21]</sup> in the presence of acetic acid to give a crude product, which contained the doubly reduced amination product in a 86:14 mixture ( $^1\text{H}$  NMR) of the two *N*-glycosyl D-*galacto* (**5a**) and L-*altro* (**5b**) derivatives, together with a small amount (about 25%) of an unknown material. After initial purification by flash chromatography, the two C-5 epimers were finally separated by HPLC and identified by NMR spectroscopy. In addition to the characteristic signals of the methyl galactopyranoside moiety, the  $^1\text{H}$  NMR spectrum of **5a** showed diagnostic signals of the azasugar ring at 3.21 and 2.20 ppm for the axial and equatorial H-1' protons, respectively, and 2.70 ppm for the H-5' proton.

The stereochemical assignment at the newly formed C-5' stereocentre was established from NMR spectroscopy. In particular, a small  $J_{4',5'}$  value (4.2 Hz) indicated a *cis* axial/equatorial relationship between the H-4' (triple quartet, 2.28 ppm) and H-5' protons (multiplet, 2.70 ppm). This was confirmed by NOE enhancements observed for H-2' and the two H-6' protons (0.9 and 1.2%, respectively) upon irradiation of the  $\text{CH}_3$  protons. Moreover, the coupling constants of the piperidine protons, particularly H-1'<sub>ax</sub>, H-1'<sub>eq</sub> and H-2', are diagnostic for the conformational assignment of **5a** and **5b** and suggest a preference for a  $^4\text{C}_1$  conformation of the azasugar ring in **5a**, whereas for **5b** the *J* values

(see Exp. Section) of the two *trans* diaxial H-4 and H-5 protons are in accordance with a  $^1\text{C}_4$  conformation.

Compared to the dicarbonyl substrates reported in the literature,<sup>[22]</sup> which belong to different stereochemical series, **3** presents other structural differences such as a C-4 methyl group instead of a hydroxy group, and two benzyloxy groups at C-2 and C-6. The diastereoselectivity of reductive amination depends on the directing effect of the hydroxy group adjacent to the C=N double bond.<sup>[22]</sup> In the reaction between **3** and **4**, the observed diastereoselectivity, which afforded a 86:14 **5a:5b** mixture, was rationalized in terms of the effect of the unique C-3 hydroxy group in directing hydride delivery, as observed in cyclic homoallylic alcohols.<sup>[23]</sup> The  $\text{NaBH}_3\text{CN}$  reductive amination reaction of the intermediate iminium ions **A** and **B** (Figure 3) is C-3 hydroxy directed, which favours the attack of the hydride to the more stable  $^2\text{H}_3$  conformer **A**, which shows one pseudoaxial group. This attack leads to a *syn* displacement of the C-4 and C-5 azasugar substituents in **5a**, whereas that on the less stable  $^3\text{H}_2$  conformer **B**, which has two axial substituents, affords **5b** as a minor product.

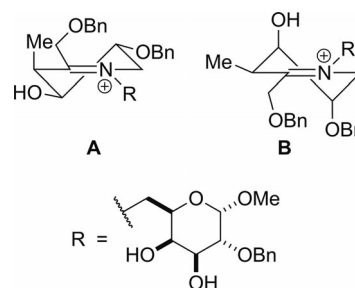


Figure 3. Structures of intermediate cyclic iminium ions.

The conversion of **5a** and **5b** into the unprotected *N*-glycosyl derivatives, **6a** and **6b**, was achieved by catalytic hydrogenation with Pd/C in methanol (Scheme 1). Spectroscopic data are in agreement with the proposed structures.

## Molecular Docking

Ligand docking is a well established computational technique that has been successfully employed in medicinal chemistry to assist drug discovery and lead optimization efforts.<sup>[24]</sup> The aim of ligand docking is to find the binding pose of a small organic molecule in a receptor pocket, and, if multiple ligands are compared, an estimate of the ligand binding affinity, referred to as the docking score. Several conformational search algorithms and scoring functions have been proposed and their performances have been compared and reviewed.<sup>[25]</sup> Among the many programs capable of performing docking simulations, AutoDock showed the best scoring function for several target proteins.<sup>[26]</sup> Moreover, although accurate prediction of the inhibition constant ( $K_i$ ) is still a difficult task, several recent papers have demonstrated that good to excellent results can be obtained by using the appropriate computational procedures.<sup>[27]</sup>

In order to optimize the design and delineate the structure–activity relationships (SARs), we investigated binding models of **6a** and **6b** and their derivatives in comparison with miglitol. Thus, taking into account the mechanism for the activity of miglitol, which has been shown to involve the inhibition of  $\alpha$ -glucosides,<sup>[28]</sup> and the X-ray structure of its complex with NtMGAM,<sup>[17]</sup> we conducted molecular docking simulations of all the investigated analogues into this catalytic pocket. The 3D structure of the NtMGAM domain complex was retrieved from the Protein Data Bank.<sup>[29]</sup> Although it has a resolution of 2.00 Å, supplementary computational manipulations were performed in order to generate a model that fitted well with MDL 73945 and can be considered “all-atom”.<sup>[30]</sup> The catalytic pocket is flexible, i.e. able to deform to fit the ligand structure, which was evidenced by changes in the volumes and surfaces<sup>[31]</sup> upon ligand inclusion with respect to its original apo form (PDB ID 2QLY)<sup>[32]</sup> when complexed with de-*O*-sulfonated kotalanol (PDB ID 3L4U),<sup>[17]</sup> acarbose (PDB ID 2QMJ),<sup>[32]</sup> casuarine (PDB ID 3CTT)<sup>[33]</sup> and miglitol (Table 1).

Table 1. Calculated volume and surface areas for selected ligand complexes with NtMGAM.

Ligand	Volume [Å <sup>3</sup> ] <sup>[a]</sup>	Surface area [Å <sup>2</sup> ] <sup>[b]</sup>
None	138.94	132.67
De- <i>O</i> -sulfonated kotalanol	159.20	151.12
Acarbose	162.99	151.31
Casuarine	169.09	156.11
Miglitol	184.30	154.03

[a] Calculations were performed by the SplitPocket web server at <http://pocket.uchicago.edu/>, see ref.<sup>[31]</sup> [b] Solvent accessible surface.

Therefore, following a tested protocol,<sup>[27a]</sup> miglitol, *N*-acetyl-D-glucosamine, glycerol and water molecules, with the exception of the two involved in hydrogen bonds with the ligand as they are present in all X-ray crystal structures of NtMGAM complexes,<sup>[17,32]</sup> were removed from the model. Successively, using the MolProbity web server,<sup>[34]</sup> the hydrogen atoms were added and the orientations of the hydroxy hydrogen atoms from the Ser, Thr and Tyr, the sulfhydryl protons of Cys and methyl protons of Met were optimized. At the same time, the positions of the hydrogen atoms on the histidine, asparagine and glutamine residues were assigned to ensure the correct ionization states. Finally, the Gasteiger–Marsili charges<sup>[35]</sup> were assigned and the whole protein with **6a**, which was protonated at nitrogen atom,<sup>[36]</sup> and with the amino sugar ring aligned analogously to that of miglitol, was optimized to an energy gradient of 0.005 kcal Å mol<sup>-1</sup> with amber 96 force field.<sup>[37]</sup> The binding models for all the compounds were constructed using that of **6a** as a template and reference ligand in the binding site.

To estimate the importance of the two water molecules present in the catalytic site, a docking study without them was also performed with miglitol as the ligand. The result showed that the importance of these two molecules is marginal ( $\Delta G_{\text{Bind}} = 0.15$  kcal mol<sup>-1</sup>), so successive studies were

conducted without them to allow the ligands to be well accommodated in the pocket.

To validate the models, we docked miglitol, casuarine and hybrid miglitol-de-*O*-sulfonated kotalanol (Figure 4), which bind to the catalytic site of NtMGAM, to compare their experimental and calculated  $K_i$  values. All the models were protonated at the azasugar nitrogen atom with the proton placed in the axial position. Equatorial protonation, results in a less stable conformer with an increased  $K_i$  value.

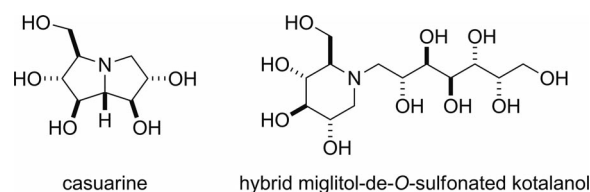


Figure 4. Structures of two analogues of miglitol.

The results reported in Table 2 show that the model is able to reproduce the experimental  $K_i$  values with a high degree of precision, which is, to the best of our knowledge, the best obtained to date with these inhibitors by the docking methodology. Although there is an inversion in the potency of casuarine respect to miglitol, which is principally due to the high flexibility of the pocket, the robustness of the approach is sufficiently secured by achievement of the correct order of magnitude.<sup>[27c]</sup>

Table 2. Calculated and experimental inhibition constants of the catalytic site of NtMGAM for miglitol and its analogues.

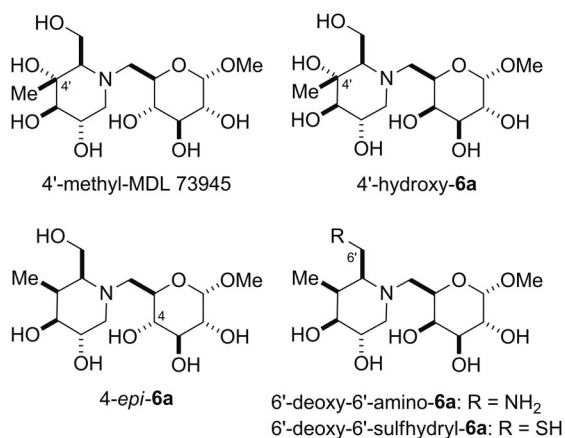
Ligand	$\Delta G_{\text{Bind}}$ calcd. [kcal mol <sup>-1</sup> ]	$K_i$ calcd. [ $\mu\text{M}$ ]	$K_i$ exp. [ $\mu\text{M}$ ]
Miglitol	-8.30	0.819	1.000 <sup>[a]</sup>
Casuarine	-8.24	0.904	0.450 <sup>[b]</sup>
Hybrid miglitol-de- <i>O</i> -sulfonated kotalanol	-7.72	2.210	1.400 <sup>[c]</sup>

[a] From ref.<sup>[17]</sup> [b] From ref.<sup>[33]</sup> [c] From ref.<sup>[38]</sup>

The model was applied to MDL 73945, **6a**, **6b** and their derivatives (Figure 5) and the results are collected in Table 3. Inspection of the results shows that 6'-deoxy-6'-amino-**6a** has the best activity among the studied compounds with an in silico  $K_i$  value of 686 pM, which, if confirmed in vitro, will be the smallest value obtained. The second lead compound, **6a**, which has a  $K_i$  value of 64 nM, has the same order of binding potency of the most recent  $\alpha$ -GIs based on the unique five-membered sulfonium ring.<sup>[39]</sup>

Compound **6b**, an epimer at C-5' with respect to **6a**, shows lower activity, as already evidenced for 5-*epi*-1-deoxynojirimycin (1-deoxy-L-idononojirimycin).<sup>[1]</sup> Protonation at the equatorial position led to a marked decrease in potency, especially for **6a**.

Regarding the SAR, the introduction of a methyl group at C-4' in MDL doubled the activity, whereas the removal of the 4'-OH led to a slight increment, which suggests the

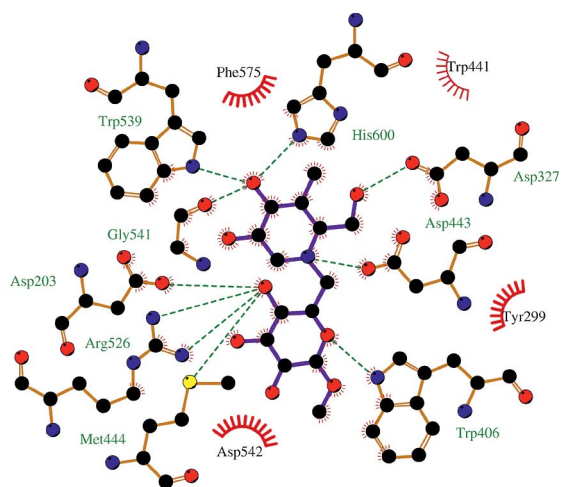
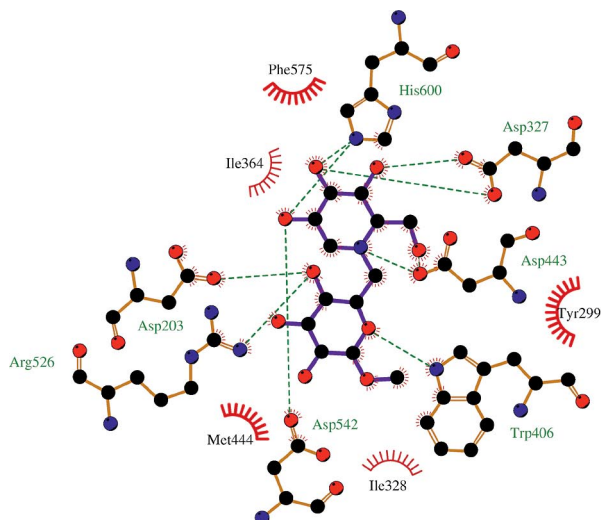
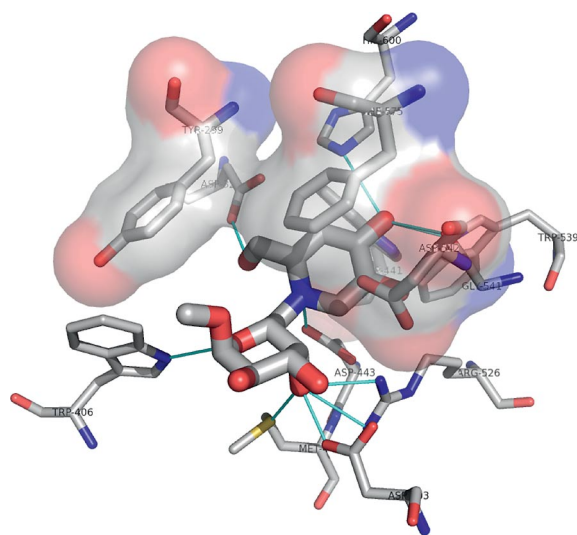
Figure 5. Structures of MDL 73945 and derivatives of **6**.Table 3. Calculated binding energies and inhibition constants for the catalytic site of NtMGAM with derivatives of **6**.

Ligand	$\Delta G_{\text{Bind}}$ calcd. [kcal mol <sup>-1</sup> ]	$K_i$ calcd. [nM]
MDL 73945	-8.92	289
4'-methyl-MDL 73945	-9.37	136
<b>6a</b>	-9.81	64
<b>6b</b>	-8.51	582
<b>6a</b> -(H <sub>eq</sub> ) <sup>[a]</sup>	-7.23	5020
<b>6b</b> -(H <sub>eq</sub> ) <sup>[a]</sup>	-8.20	976
4'-hydroxy-6a	-9.63	87
4-epi-6a	-9.54	101
6'-deoxy-6'-sulfhydryl-6a	-10.41	23
6'-deoxy-6'-amino-6a	-12.51	0.680

[a] With the nitrogen azasugar protonated equatorially.

great importance of hydrophobic interactions. Moreover, the epimerization of 4-OH led to the formation of other two hydrogen bonds, which slightly increased the activity and further stressed the marginal importance of these types of interactions. All hydrophobic and hydrogen bonding interactions present in MDL 73945 and **6a** are depicted in Figure 6. For **6a**, a more realistic 3D picture is also shown (Figure 7). From the two figures, a new hydrophobic interaction emerges between the methyl group in **6a** and Trp441. Moreover, the presence of ten hydrogen bonds is noted; four of them to Asp203, Arg256 and Met444, due to the axial position of 4-OH. However, these four bonds are reduced to two when the same hydroxy group is in the equatorial position.

Finally, Figure 8 reports the superposition of miglitol, MDL 73945 and **6a** for a better comparison between the conformations and positions adopted upon binding. In the case of miglitol and MDL 73945, the azasugar rings are almost perfectly superimposed, whereas for **6a** the introduction of an axial methyl group at C-4' implies a notable shift of this portion, which forces the protonated nitrogen atom sufficiently close to Asp443 in the catalytic residue to engage in a hydrogen bond essential for inhibitory activity.<sup>[1]</sup> The second glycosidic rings occupy almost the same position in the +1 site.

Figure 6. 2D schematic view of hydrogen bonds and hydrophobic interactions for MDL 73945 (top) and **6a** (bottom) docked in NtMGAM (prepared with LigPlot<sup>+</sup>).<sup>[19]</sup>Figure 7. Molecular docking result with **6a** at the catalytic site of NtMGAM. Only the amino acid residues effectively involved are shown for clarity. The ligand is represented as a tube. Turquoise lines represent hydrogen bonds between the ligand and receptor.

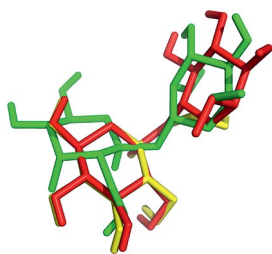


Figure 8. Superposition of some ligands docked at the NtMGAM catalytic site. Only polar hydrogen atoms are represented for clarity. Ligands are rendered as sticks with the following colour code: miglitol yellow, MDL 73945 red, **6a** green.

### X-ray Diffraction Study

The results obtained for **6a** and **6b** prompted us to pursue their complete characterization. Unfortunately, the very small amount of available product prevented any crystallization attempts. As a consequence, we tried to predict their crystal structures.

Crystal structure prediction has been increasingly addressed in the last few years.<sup>[40]</sup> Although this task is an old chemists' dream,<sup>[41]</sup> only the good results of the last decade<sup>[42]</sup> allow us to trust in the computational approaches available. The general scepticism around this prevision technique<sup>[43]</sup> is counterbalanced by its results, which are of great help towards understanding as yet unknown structure–property relationships. The results proposed in this work, although inferred by means of technically rigorous methods, must be considered as one of the most probable solutions. More specifically, given the great number of predicted structures, the whole process actually results in polymorph prediction,<sup>[44]</sup> i.e. in the prediction of different unit cells for the same chemical formula. Moreover, these results can be particularly useful in case of future availability of greater amounts of products: they can be the starting models for their complete XRPD characterization.

The computational approach is described in detail in the experimental section. The choice of space groups (SGs) to be considered suitable for the crystallization of **6a** and **6b** was simplified by considering that both compounds are optically active and can crystallize in chiral SGs only – the so called Sohncke SGs – which contain only rotation and screw axes. As a consequence of the 230 possible SGs “only” 65 were initially considered. Although more than the 70% of organic compounds crystallize in  $P2_12_12_1$  and  $P2_1$  SGs,<sup>[45]</sup> the search for possible SGs was extended to all the potential chiral candidates. The predicted SGs partially respect Baur and Kassner<sup>[45]</sup> statistics, as **6a** crystallizes in orthorhombic  $P2_12_12$  and two different polymorphs, a monoclinic  $P2_1$  and an orthorhombic  $P2_12_12_1$ , were chosen as SGs for **6b** (Figure 9).

The most probable SG was selected by finding the lowest energy packing. In the case of very close energy values, the packing efficiency<sup>[46]</sup> was chosen as a second parameter to choose the best SG. As a consequence, structures with higher densities were selected.

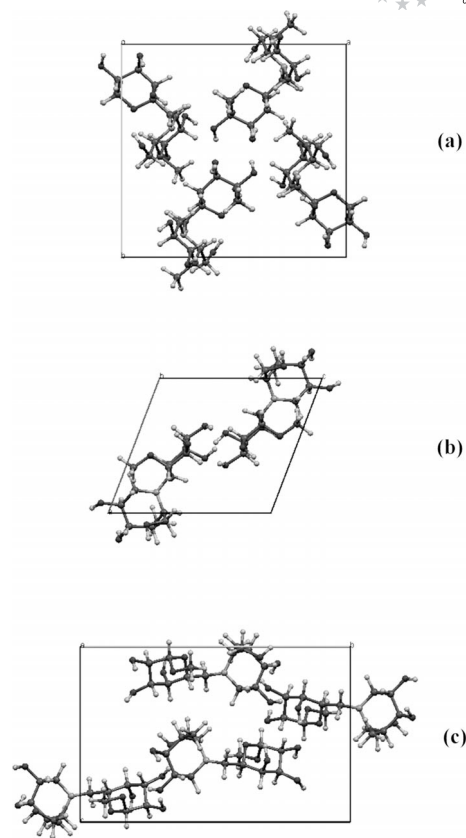


Figure 9. The orthorhombic cell of **6a** viewed along the  $c$  axis (a). The monoclinic (b) and orthorhombic (c) cells of **6b** viewed along the  $b$  and  $a$  axes, respectively.

The most relevant structural parameters are reported for **6a** and **6b** in Table 4. The proposed crystal structures show a great number of hydrogen bonds, which play a key role in the overall stabilization of the asymmetric units in the unit cell. The chosen orthorhombic structure of **6a** is energetically favoured over the other proposed polymorphic structures of the same set. The energy differences between the computed structures is relevant – more than  $0.54 \text{ kcal mol}^{-1} \text{ asymmetric cell}^{-1}$  – thus confirming the proposed structure as the only real candidate. This is not true for **6b**, where the energy difference between the potential candidates is small enough to suggest a coexistence of two

Table 4. The cell parameters **6a** and **6b** (without their standard uncertainties, as a result of the exact calculated values).

	<b>6a</b>	<b>6b</b>	
Crystal system	orthorhombic	monoclinic	orthorhombic
Space group	$P2_12_12$	$P2_1$	$P2_12_12_1$
$a$ [Å]	14.9106	9.6022	7.7820
$b$ [Å]	14.1663	7.6416	17.8721
$c$ [Å]	7.8184	10.7755	11.6472
$\alpha$ [°]	90	90	90
$\beta$ [°]	90	110.8101	90
$\gamma$ [°]	90	90	90
Volume [Å <sup>3</sup> ]	1651.47	739.084	1511.95
Energy [kcal mol <sup>-1</sup> asymmetric cell <sup>-1</sup> ]	0.301	0.722	0.736
Density [mg m <sup>-3</sup> ]	1.357	1.516	1.482

different crystal structures. Interestingly, for all three candidates, the total puckering amplitudes ( $Q$ ), calculated as specified elsewhere,<sup>[47]</sup> are very similar (Table 5).

Table 5. Total puckering amplitude ( $Q$ ) for **6a** and **6b**. Ring a is the six-membered ring with an oxygen atom, and ring b is the six-membered ring with a nitrogen atom.

		<b>6a</b>	<b>6b</b>	
		orthorhombic	monoclinic	orthorhombic
$Q$	Ring a	0.5948	0.5776	0.6053
$Q$	Ring b	0.5805	0.5480	0.5301

This result suggests that, in spite of the different packing characteristics, the molecules with the same absolute configuration are almost superimposable. This is not obvious in the solid state, where the great number of interactions, compared to less dense phases, usually force the unit cell building blocks to adopt different conformations.

## Conclusions

We have reported the design, based on molecular docking studies, and synthesis of new *N*-glycosyl-derived analogues of MDL 73945, a potential  $\alpha$ -GI with a  $K_i$  value of 64 nM. A more potent derivative 6'-deoxy-6'-amino-**6a** was also isolated and its further synthesis and biological screening are in progress. The results obtained by SAR analysis can be applied to further manipulation of the most recent  $\alpha$ -GIs based on the five-membered sulfonium ring. Further investigations will be devoted towards the study of new reactions of **3** and other  $\delta$ -dicarbonyl sugar homologues with different 6-amino sugar derivatives and nonsaccharidic amines with the aim to find even better performing compounds. Moreover, the future availability of larger quantities of the synthesized compounds could enable their crystallization and therefore their complete characterization through XRPD. As a consequence, the unit cells reported above for **6a** and **6b** could help to index the X-ray patterns.

## Experimental Section

**General:** Melting points were determined with a Kofler hot-stage apparatus. Optical rotations were measured with a Perkin-Elmer 241 polarimeter at 20  $\pm$  2 °C. All reactions were followed by TLC with Kieselgel 60 F<sub>254</sub> with detection by UV light and/or with ethanolic 10% sulfuric acid and heating. Kieselgel 60 was used for column and flash chromatography (E. Merck, 70–230 and 230–400 mesh, respectively). <sup>1</sup>H NMR spectra were recorded with a Varian VnmrJ instrument at 500 MHz with Me<sub>4</sub>Si as the internal standard. <sup>13</sup>C NMR spectra were recorded at 50 MHz. Assignments were made, when possible, with the aid of DEPT experiments for comparison with values for known compounds. HRMS were recorded with a VG ZAB-2SE double focussing magnetic sector mass spectrometer operating at 70 eV. Hydrogenation reactions were performed with a Parr® apparatus. HPLC purifications were made with a Microsorb silica Dinamax-100 Å preparative column (250  $\times$  21 mm) at a flow rate of 21 mL min<sup>-1</sup> with a Varian Pro

Star instrument. Solvents were dried by distillation according to standard procedures,<sup>[48]</sup> and stored over molecular sieves (4 Å), which were activated for at least 24 h at 400 °C. Na<sub>2</sub>SO<sub>4</sub> was used as the drying agent for solutions.

**Starting Materials:** Cyclopropyl lactose adduct **1**<sup>[14]</sup> and 6-amino-6-deoxy- $\alpha$ -D-galactopyranoside **4**,<sup>[21]</sup> were prepared according to the reported methods.

**Reductive Amination of 3:** To a stirring solution of **4** (720 mg, 2.23 mmol) and CH<sub>3</sub>CO<sub>2</sub>H (0.13 mL, 2.23 mmol) in dry MeOH (25 mL) at -78 °C was added a solution of **3** (990 mg, 2.78 mmol) in dry MeOH (25 mL) over about 15 min followed by NaBH<sub>3</sub>CN (350 mg, 5.60 mmol) in MeOH (20 mL) under nitrogen atmosphere. The reaction mixture was stirred for 2 h at -78 °C and then for 48 h at room temp., when the disappearance of the starting products was confirmed (TLC monitoring). The solvent was removed at reduced pressure and the residue was treated with a saturated aqueous solution of Na<sub>2</sub>CO<sub>3</sub> (10 mL). The solution was extracted into CH<sub>2</sub>Cl<sub>2</sub> (3  $\times$  10 mL) and the organic phases were dried with Na<sub>2</sub>SO<sub>4</sub>. After filtration, the solvent was evaporated at reduced pressure, and the crude was purified by flash chromatography (Cy/AcOEt 50%) to afford a syrup, which comprised a 84:16 mixture of **5a** and **5b** (75% yield). This anomeric mixture was then purified by HPLC (*n*-hexane/2-propanol 90:10) to afford pure **5a** ( $t_R$  = 12 min) and **5b** ( $t_R$  = 19 min).

***N*-(6-Deoxy-1-*O*-methyl-6- $\alpha$ -D-galactopyranosyl)-2,6-di-*O*-benzyl-1,4-dideoxy-4-*C*-methyl-galacto-nojirimycin (5a):** 63.3% yield.  $[\alpha]_D^{25}$  = -64.5 ( $c$  = 1.21, CHCl<sub>3</sub>). <sup>1</sup>H NMR (500 MHz, CDCl<sub>3</sub>, 27 °C):  $\delta$  = 0.92 (d,  $J$  = 7.2 Hz, 3 H, Me), 2.20 (dd,  $J$  = 7.3, 12.0 Hz, 1 H, 1'-a-H), 2.28 (tq,  $J$  = 4.2, 7.2 Hz, 1 H, 4'-H), 2.70 (m, 1 H, 5'-H), 2.71 (m, 1 H, 6a-H), 3.00 (dd,  $J$  = 10.5, 12.5 Hz, 1 H, 6b-H), 3.21 (dd,  $J$  = 3.7, 12.0 Hz, 1 H, 1'-b-H), 3.29 (t,  $J$  = 9.2 Hz, 1 H, 4-H), 3.34 (s, 3 H, OMe), 3.45 (dt,  $J$  = 3.7, 7.3 Hz, 1 H, 2'-H), 3.49 (dd,  $J$  = 3.8, 9.2 Hz, 1 H, 2-H), 3.55 (dd,  $J$  = 4.2, 7.3 Hz, 1 H, 3'-H), 3.57–3.61 (m, 3 H, 6'-H and 5-H), 3.72 (t,  $J$  = 9.2 Hz, 1 H, 3-H), 4.47 (d,  $J$  = 11.8 Hz, 1 H, C-2-OCH<sub>2</sub>Ph), 4.51 (d,  $J$  = 11.8 Hz, 1 H, C-2-OCH<sub>2</sub>Ph), 4.59 (d,  $J$  = 11.7 Hz, 1 H, C-6-OCH<sub>2</sub>Ph), 4.60 (d,  $J$  = 11.7 Hz, 1 H, C-6-OCH<sub>2</sub>Ph), 4.67 (d,  $J$  = 3.8 Hz, 1 H, 1-H), 7.25–7.35 (m, 10 H, aromatic H) ppm. <sup>13</sup>C NMR (125 MHz, CDCl<sub>3</sub>, 27 °C):  $\delta$  = 10.1 (Me), 35.9 (C-4'), 54.0 (C-1'), 55.4 (OMe), 56.8 (C-6), 62.3 (C-5'), 65.5 (C-5), 69.7 (C-6'), 71.8 (C-2), 72.1 (CH<sub>2</sub>Ph), 72.7 (C-3'), 73.4 (CH<sub>2</sub>Ph), 73.6 (C-3), 76.0 (C-4), 76.3 (C-2'), 99.4 (C-1), 127.8, 127.9, 128.1, 128.4, 128.5, 128.6 (aromatic CH), 137.3, 138.2 (aromatic C) ppm. HRMS: calcd. for C<sub>28</sub>H<sub>39</sub>NO<sub>8</sub> [M]<sup>+</sup> 517.6111; found 517.6110.

***N*-(6-Deoxy-1-*O*-methyl-6- $\alpha$ -D-galactopyranosyl)-2,6-di-*O*-benzyl-1,4-dideoxy-4-*C*-methyl-*altro*-nojirimycin (5b):** 11.7% yield.  $[\alpha]_D^{25}$  = +18 ( $c$  = 1.13, CHCl<sub>3</sub>). <sup>1</sup>H NMR (500 MHz, CDCl<sub>3</sub>, 27 °C):  $\delta$  = 0.86 (d,  $J$  = 6.9 Hz, 3 H, Me), 2.11 (dd,  $J$  = 4.2, 12.0 Hz, 1 H, 1'-a-H), 2.18 (ddq,  $J$  = 5.4, 6.9, 8.4 Hz, 1 H, 4'-H), 2.90 (m, 1 H, 6a-H), 2.94 (m, 1 H, 5'-H), 3.21 (t,  $J$  = 9.2 Hz, 1 H, 4-H), 3.22 (dd,  $J$  = 3.1, 12.0 Hz, 1 H, 1'-b-H), 3.25 (s, 3 H, OMe), 3.42 (dd,  $J$  = 10.3, 12.4 Hz, 1 H, 6b-H), 3.46 (dt,  $J$  = 3.1, 4.2 Hz, 1 H, 2'-H), 3.53 (dd,  $J$  = 3.8, 9.6 Hz, 1 H, 2-H), 3.93 (dd,  $J$  = 4.2, 5.4 Hz, 1 H, 3'-H), 3.53–3.58 (m, 3 H, 6'-H and 5-H), 3.82 (t,  $J$  = 9.2 Hz, 1 H, 3-H), 4.42 (d,  $J$  = 11.7 Hz, 1 H, C-2-OCH<sub>2</sub>Ph), 4.49 (d,  $J$  = 11.7 Hz, 1 H, C-2-OCH<sub>2</sub>Ph), 4.51 (d,  $J$  = 4.8 Hz, 1 H, 1-H), 4.59 (d,  $J$  = 11.6 Hz, 1 H, C-6-OCH<sub>2</sub>Ph), 4.64 (d,  $J$  = 11.6 Hz, 1 H, C-6-OCH<sub>2</sub>Ph), 7.25–7.35 (m, 10 H, aromatic H) ppm. <sup>13</sup>C NMR (125 MHz, CDCl<sub>3</sub>, 27 °C):  $\delta$  = 7.1 (Me), 37.3 (C-4'), 46.5 (C-1'), 55.1 (OMe), 56.2 (C-6), 62.9 (C-5'), 66.9 (C-5), 67.9 (C-6'), 71.8 (C-3'), 71.9 (C-3), 72.3 (CH<sub>2</sub>Ph), 72.5 (C-4), 73.4 (CH<sub>2</sub>Ph), 74.6 (C-2), 75.3 (C-2'), 100.9 (C-1), 127.5, 128.1, 128.3, 128.5, 128.9,

129.2 (aromatic CH), 137.0, 137.9 (aromatic C) ppm. HRMS: calcd. for  $C_{28}H_{39}NO_8$   $[M]^+$  517.6111; found 517.6109.

**Debenzylation of 5a and 5b:** To a solution of **5** (60 mg 0.11 mmol) in MeOH (2 mL) was added a spatula tip of 10% Pd/C and the suspension was shaken on a Parr apparatus under hydrogen (90 psi) for 36 h. The reaction mixture was filtered through Celite, and the filtrate was evaporated at reduced pressure to afford a crude, which was purified by flash chromatography ( $CH_3OH/CH_2Cl_2/H_2O$ , 4:2:1) to afford **6a** and **6b**.

**N-(6-Deoxy-1-O-methyl-6- $\alpha$ -D-galactopyranosyl)-1,4-dideoxy-4-C-methyl-galacto-nojirimycin (6a):** 85% yield, colourless crystals; m.p. 139–140 °C.  $[a]_D^{25} = -31$  ( $c = 1.03$ ,  $CHCl_3$ ).  $^1H$  NMR (500 MHz,  $CDCl_3$ , 27 °C):  $\delta = 0.94$  (d,  $J = 7.0$  Hz, 3 H, Me), 2.22 (tq,  $J = 4.5$ , 7.0 Hz, 1 H, 4'-H), 2.26 (dd,  $J = 10.1$ , 11.6 Hz, 1 H, 1'a-H), 2.61 (ddd,  $J = 5.0$ , 5.8, 7.0 Hz, 1 H, 5'-H), 2.62 (dd,  $J = 6.5$ , 14.1 Hz, 1 H, 6a-H), 2.99 (dd,  $J = 9.2$ , 14.1 Hz, 1 H, 6b-H), 3.18 (t,  $J = 9.2$  Hz, 1 H, 4-H), 3.22 (dd,  $J = 4.5$ , 11.6 Hz, 1 H, 1'b-H), 3.36 (dd,  $J = 3.8$ , 9.7 Hz, 1 H, 2-H), 3.38 (dd,  $J = 4.5$ , 7.9 Hz, 1 H, 3'-H), 3.42 (s, 3 H, OMe), 3.59 (t,  $J = 9.2$  Hz, 1 H, 3-H), 3.61 (ddd,  $J = 4.5$ , 7.9, 10.1 Hz, 1 H, 2'-H), 3.63 (dd,  $J = 5.0$ , 11.5 Hz, 1 H, 6'a-H), 3.69 (dt,  $J = 6.5$ , 9.2 Hz, 5-H), 3.85 (dd,  $J = 5.8$ , 11.5 Hz, 1 H, 6'b-H), 4.63 (d,  $J = 3.8$  Hz, 1 H, 1-H) ppm.  $^{13}C$  NMR (125 MHz,  $CDCl_3$ , 27 °C):  $\delta = 9.1$  (Me), 37.1 (C-4'), 54.6 (C-6), 55.7 (OMe), 56.2 (C-1'), 62.0 (C-6'), 65.8 (C-5'), 69.0 (C-2'), 70.0 (C-5), 73.2 (C-2), 74.5 (C-3), 75.2 (C-4), 76.0 (C-3'), 101.1 (C-1) ppm. HRMS: calcd. for  $C_{14}H_{27}NO_8$   $[M]^+$  337.3660; found 337.3659.

**N-(6-Deoxy-1-O-methyl-6- $\alpha$ -D-galactopyranosyl)-1,4-dideoxy-4-C-methyl-altro-nojirimycin (6b):** 83% yield, colourless crystals; m.p. 125–127 °C.  $[a]_D^{25} = +20$  ( $c = 0.98$ ,  $CHCl_3$ ).  $^1H$  NMR (500 MHz,  $CDCl_3$ , 27 °C):  $\delta = 0.90$  (d,  $J = 7.0$  Hz, 3 H, Me), 2.14 (ddq,  $J = 5.3$ , 7.0, 8.6 Hz, 1 H, 4'-H), 2.20 (dd,  $J = 9.9$ , 11.5 Hz, 1 H, 1'a-H), 2.75–2.79 (m, 2 H, 5'-H, 6a-H), 2.96 (dd,  $J = 4.8$ , 11.5 Hz, 1 H, 1'b-H), 3.12 (t,  $J = 7.5$  Hz, 1 H, 4-H), 3.25 (dd,  $J = 9.0$ , 13.6 Hz, 1 H, 6b-H), 3.29 (s, 3 H, OMe), 3.45 (dd,  $J = 4.8$ , 9.0 Hz, 1 H, 2-H), 3.63 (ddd,  $J = 4.8$ , 7.9, 9.9 Hz, 1 H, 2'-H), 3.70 (dd,  $J = 7.5$ , 9.0 Hz, 1 H, 3-H), 3.77 (dd,  $J = 5.3$ , 7.9 Hz, 1 H, 3'-H), 3.79–3.84 (m, 3 H, 5-H, 6'-H), 4.45 (d,  $J = 4.8$  Hz, 1 H, 1-H) ppm.  $^{13}C$  NMR (125 MHz,  $CDCl_3$ , 27 °C):  $\delta = 8.5$  (Me), 37.2 (C-4'), 52.2 (C-1'), 54.1 (C-6), 55.0 (OMe), 60.1 (C-6'), 65.9 (C-5'), 67.8 (C-2'), 71.7 (C-5), 72.0 (C-4), 72.7 (C-3), 75.4 (C-2), 75.8 (C-3'), 102.6 (C-1) ppm. HRMS: calcd. for  $C_{14}H_{27}NO_8$   $[M]^+$  337.3660; found 337.3661.

**Molecular Docking:** Computational docking was carried out by applying the Lamarckian genetic algorithm implemented in AutoDock 4.2.3.<sup>[49]</sup> For fine docking we used the following parameters: grid spacing 0.260 Å, number of runs 100, npts = 70 70 70 centred on **6a**, ga\_num\_evals = 25000000, ga\_pop\_size = 150 and ga\_num\_generations 27000. The graphical user interface AutoDockTools (1.5.6rc1, R45)<sup>[50]</sup> was used to establish the Autogrid points and visualize docked ligand–nucleic acid structures.

**In silico Crystal Structure Prediction:** Crystal structure prediction was performed using the Polymorph module present in Accelrys Materials Studio 4.4.<sup>[51]</sup> The starting molecular structures were geometrically and energetically optimized by spin restricted B88 DFT calculations<sup>[52]</sup> exchange and LYP<sup>[53]</sup> correlation as implemented in DMol<sup>3</sup>.<sup>[51]</sup> Monte Carlo simulated annealing, which consisted of 10000 steps and a 0.025 heating factor in a temperature range 300–150000 K, was used to explore the lattice energy hypersurfaces for potential crystal packing solutions. Thousands of possible answers were clustered to remove duplicates and speed up the geometry optimization of each unique structure. This task was performed

using Compass Force Field<sup>[54]</sup> and Smart algorithm (Convergence tolerance: energy:  $2 \times 10^{-5}$  kcalmol<sup>-1</sup>, force: 0.001 kcalmol<sup>-1</sup> Å<sup>-1</sup>, stress: 0.001 GPa, displacement:  $1 \times 10^{-5}$  Å). After a second clustering step, the final structures were ranked on the basis of their lattice energies.

All the consistent forcefields (CFF91, CFF, pcff, COMPASS) available in Accelrys Materials Studio 4.4<sup>[48]</sup> have the same functional form, which differ mainly for parameter values. They are considered to be an improvement on the classical force fields (AMBER or CHARMM) and therefore often called second-generation force fields. Atom equivalences for the assignment of parameters to force field types and some combination rules for nonbonded terms may also differ. COMPASS (Condensed-phase Optimized Molecular Potentials for Atomistic Simulation Studies) is a force field expressly projected to support atomistic simulations of condensed phase materials and it is the first ab initio force field that has been parameterized and validated using condensed-phase properties as well as various ab initio and empirical data for molecules in isolation.<sup>[55]</sup>

Its parameterization procedure can be divided into two phases: ab initio parameterization and empirical optimization. In the first phase, partial charges and valence parameters were derived by fitting to ab initio potential energy surfaces. At this point, the van der Waals parameters were fixed to a set of initial approximated parameters. In the second phase, force field optimization was carried out in order to yield a good agreement with experimental data. A few critical valence parameters were adjusted based on the gas phase experimental data. More importantly, the van der Waals parameters were optimized to fit the condensed-phase properties.

**Supporting Information** (see footnote on the first page of this article): A file containing **6a** and **6b** calculated cif files is available. Those cif files do not correspond to experimentally derived structure and therefore are not deposited at the CCDC.

- [1] E. Borges de Melo, A. Gomes da Silvera, I. Carvalho, *Tetrahedron* **2006**, *62*, 10277–10302.
- [2] a) K. M. Robinson, M. E. Begovic, B. L. Rhinehart, E. W. Heinke, J. B. Ducep, P. R. Kastner, F. N. Marshall, C. Danzin, *Diabetes* **1991**, *40*, 825–830; b) R. A. Dwek, T. D. Butters, F. M. Platt, N. N. Zitzmann, *Nat. Rev. Drug Discovery* **2002**, *1*, 65–75; c) P. Hollander, X. Pi-Sunyer, R. E. Coniff, *Diabetes Care* **1997**, *20*, 248–253; d) F. Marcelo, Y. He, S. A. Yuzva, L. Nieto, J. Jiménez-Barbero, M. Sollogoub, D. J. Voadlo, G. D. Davies, Y. Blériot, *J. Am. Chem. Soc.* **2009**, *131*, 5390–5392; e) K. Martínez-Mayorga, J. L. Medina-Franco, S. Mari, F. J. Cañada, E. Rodríguez-García, P. Vogel, H. Li, Y. Blériot, P. Sinaÿ, J. Jiménez-Barbero, *Eur. J. Org. Chem.* **2004**, *20*, 4119–4129.
- [3] C. P. Kordik, A. B. Reitz, *J. Med. Chem.* **1999**, *42*, 181–201.
- [4] a) N. Asano, *Glycobiology* **2003**, *13*, 93R–104R; b) J. Alper, *Science* **2001**, *291*, 2338–2343; c) T. D. Butters, R. A. Dwek, F. M. Platt, *Chem. Rev.* **2000**, *100*, 4683–4696.
- [5] a) Y. Nishimura, T. Satoh, H. Adachi, S. Kondo, T. Takeuchi, M. Azetaka, H. Fukuyasu, Y. Iizuka, *J. Med. Chem.* **1997**, *40*, 2626–2633; b) N. Zitzmann, A. S. Mehta, S. Carrouée, T. D. Butters, F. M. Platt, J. McCauley, B. S. Blumberg, R. A. Dwek, T. M. Block, *Proc. Natl. Acad. Sci. USA* **1999**, *96*, 11878–11882.
- [6] a) P. Chand, P. L. Kotian, A. Dehghani, Y. El-Kattan, T.-H. Lin, T. L. Hutchison, Y. Sudhakar Babu, S. Bantia, A. J. Eliott, J. A. Montgomery, *J. Med. Chem.* **2001**, *44*, 4379–4392; b) C. U. Kim, W. Lew, M. A. Williams, H. Liu, L. Zhang, S. Swaminathan, N. Bischofberger, M. S. Chen, D. B. Mendel,

- C. Y. Tai, W. G. Laver, R. C. Stevens, *J. Am. Chem. Soc.* **1997**, *119*, 681–690.
- [7] A. da S. Gomes, C. H. T. P. Silva, V. B. da Silva, I. Carvalho, *Curr. Bioact. Compd.* **2009**, *5*, 99–109.
- [8] H. S. Yee, N. T. Fong, *Pharmacotherapy* **1996**, *16*, 792–805.
- [9] X. Chen, Y. Zheng, Y. Shen, *Biotechnol. Prog.* **2005**, *21*, 1002–1003.
- [10] a) M. Yusuke, T. Koji, H. Masatoshi, *Mol. Cell Pharm.* **2009**, *1*, 188–192; b) S. Horii, H. Fukase, T. Matsuo, Y. Kameda, N. Asano, K. Matsui, *J. Med. Chem.* **1986**, *29*, 1038–1046.
- [11] a) K. Matsumoto, M. Yano, S. Miyake, Y. Ueki, Y. Yamaguchi, S. Akazawa, Y. Tominaga, *Diabetes Care* **1998**, *21*, 256–260; b) N. Asano, R. J. Nash, R. J. Molyneux, G. W. J. Fleet, *Tetrahedron: Asymmetry* **2000**, *11*, 1645–1680; c) M. Bollen, A. Vandebroek, W. Stalmans, *Biochem. Pharmacol.* **1988**, *37*, 905–909; d) ; P. Compain, O. R. Martin, in: *Iminosugars: From Synthesis to Therapeutic Applications* (Eds.: P. Compain O. R. Martin), John Wiley & Sons, West Sussex, England, **2007**; e) P. C. Tyler, B. G. Winchester, in: *Iminosugars as Glycosidase Inhibitors: Nojirimycin and Beyond* (Ed.: A. E. Stütz), Wiley-VCH, Weinheim, **1999**, pp. 125–155; f) T. D. Butters, R. A. Dwek, F. M. Platt, *Curr. Top. Med. Chem.* **2003**, *3*, 561–574.
- [12] J. B. Ducep; C. Danzin, *Eur. Pat. Appl.* **1989**, EP 344383.
- [13] P. L. Barili, G. Berti, G. Catelani, F. D'Andrea, F. De Rensis, L. Puccioni, *Tetrahedron* **1997**, *53*, 3407–3416.
- [14] A. Corsaro, U. Chiacchio, R. Adamo, V. Pistarà, A. Rescifina, R. Romeo, G. Catelani, F. D'Andrea, M. Mariani, E. Attolino, *Tetrahedron* **2004**, *60*, 3787–3795.
- [15] a) P. L. Barili, G. Berti, G. Catelani, F. D'Andrea, *Gazz. Chim. Ital.* **1992**, *122*, 135–142; b) G. Catelani, A. Corsaro, F. D'Andrea, M. Mariani, V. Pistarà, E. Vittorino, *Carbohydr. Res.* **2003**, *338*, 2349–2358.
- [16] a) V. Pistarà, P. L. Barili, G. Catelani, A. Corsaro, F. D'Andrea, S. Fisichella, *Tetrahedron Lett.* **2000**, *41*, 3253–3256; b) G. Catelani, A. Corsaro, F. D'Andrea, M. Mariani, V. Pistarà, *Bioorg. Med. Chem. Lett.* **2002**, *12*, 3312–3315.
- [17] L. Sim, K. Jayakanthan, S. Mohan, R. Nasi, B. D. Johnston, B. M. Pinto, D. R. Rose, *Biochemistry* **2010**, *49*, 443–451.
- [18] G. J. Davies, K. S. Wilson, B. Henrissat, *Biochem. J.* **1997**, *321*, 557–559.
- [19] A. C. Wallace, R. A. Laskowski, J. M. Thornton, *Protein Eng.* **1996**, *8*, 127–134.
- [20] V. Pistarà, A. Corsaro, A. Rescifina, G. Catelani, F. D'Andrea, *XII Convegno-Scuola sulla Chimica dei Carboidrati*, Pontignano (SI), **2010**, PC-6.
- [21] M. Landi, G. Catelani, F. D'Andrea, E. Ghiaini, G. Amari, P. Puccini, N. Bianchi, R. Gambari, *Eur. J. Med. Chem.* **2009**, *44*, 745–754.
- [22] a) E. W. Baxter, A. B. Reitz, *J. Org. Chem.* **1994**, *59*, 3175–3185; b) D. D. Dhavale, N. N. Saha, V. N. Desai, *J. Org. Chem.* **1997**, *64*, 7482–7484.
- [23] A. H. Hoveyda, D. A. Evans, G. C. Fu, *Chem. Rev.* **1993**, *93*, 1307–1370.
- [24] D. B. Kitchen, H. Decornez, J. R. Furr, J. Bajorath, *Nat. Rev. Drug Discovery* **2004**, *3*, 935–949.
- [25] a) I. Halperin, B. Ma, H. Wolfson, R. Nussinov, *Proteins Struct., Funct., Bioinf.* **2002**, *47*, 409–443; b) B. D. Bursulaya, M. Totrov, R. Abagyan, C. L. Brooks III, *J. Comput.-Aided Mol. Des.* **2003**, *17*, 755–763.
- [26] H. Park, J. Lee, S. Lee, *Proteins Struct., Funct., Bioinf.* **2006**, *65*, 549–554.
- [27] a) F. Mazué, D. Colin, J. Gobbo, M. Wegner, A. Rescifina, C. Spatafora, D. Fasseur, D. Delmas, P. Meunier, C. Tringali, N. Latruffe, *Eur. J. Med. Chem.* **2010**, *45*, 2972–2980; b) H. Sadeghian, A. Sadeghian, M. Pordel, M. Rahimizadeh, P. Jahandari, A. Orafaie, M. Bakavoli, *Med. Chem. Res.* **2010**, *19*, 103–119; c) M. Mladenović, N. Vuković, S. Sukdolak, S. Solujić, *Molecules* **2010**, *15*, 4294–4308; d) V. M. Popov, W. A. Yee, A. C. Anderson, *Proteins Struct., Funct., Bioinf.* **2007**, *66*, 375–387; e) K. Yelekçi, Ö. Karahan, M. Toprakçi, *J. Neural Transm.* **2007**, *114*, 725–732; f) M. Toprakçi, K. Yelekçi, *Bioorg. Med. Chem. Lett.* **2005**, *15*, 4438–4446; g) E. Jenwitheesuk, R. Samudrala, *Antiviral Ther.* **2005**, *10*, 157–166; h) R. Ragno, A. Mai, G. Sbardella, M. Artico, S. Massa, C. Musiu, M. Mura, F. Marturana, A. Cadeddu, P. La Colla, *J. Med. Chem.* **2004**, *47*, 928–934; i) D.-F. Wang, O. Wiest, P. Helquist, H.-Y. Lan-Hargest, N. L. Wiech, *J. Med. Chem.* **2004**, *47*, 3409–3417; j) O. G. Dadrass, A. M. Sobhani, A. Shafiee, M. Mahmoudian, *Daru J. Fac. Pharm. Tehran Univ. Med. Sci.* **2004**, *12*, 1–10.
- [28] P. H. Joubert, H. L. Venter, G. N. Foukaridis, *Brit. J. Clin. Pharmacol.* **1990**, *30*, 391–396.
- [29] <http://www.rcsb.org/PDB>, code 3L4W.
- [30] T. L. Nguyen, C. McGrath, A. R. Hermone, J. C. Burnett, D. W. Zaharevitz, B. W. Day, P. Wipf, E. Hamel, R. Gussio, *J. Med. Chem.* **2005**, *48*, 6107–6116.
- [31] Y. Y. Tseng, C. Dupree, Z. J. Chen, W.-H. Li, *Nucleic Acids Res.* **2009**, *37*, W384–W389.
- [32] L. Sim, R. Quezada-Calvillo, E. E. Sterchi, B. L. Nichols, D. R. Rose, *J. Mol. Biol.* **2008**, *375*, 782–792.
- [33] F. Cardona, C. Parmeggiani, E. Faggi, C. Bonaccini, P. Gratteri, L. Sim, T. M. Gloster, S. Roberts, G. J. Davies, D. R. Rose, A. Goti, *Chem. Eur. J.* **2009**, *15*, 1627–1636.
- [34] V. B. Chen, W. B. Arendall III, J. J. Headd, D. A. Keedy, R. M. Immormino, G. J. Kapral, L. W. Murray, J. S. Richardson, D. C. Richardson, *Acta Crystallogr., Sect. D: Biol. Crystallogr.* **2010**, *66*, 12–21; <http://molprobity.biochem.duke.edu>.
- [35] J. Gasteiger, M. Marsil, *Tetrahedron Lett.* **1978**, *34*, 3181–3184.
- [36] A. E. Stutz, in: *Iminosugars as Glycosidase Inhibitors: Nojirimycin and Beyond*, Wiley-VCH, Weinheim, Germany, **1999**.
- [37] W. D. Cornell, P. Cieplak, C. I. Bayly, I. R. Gould, K. M. Merz Jr, D. M. Ferguson, D. C. Spellmeyer, T. Fox, J. W. Caldwell, P. A. Kollman, *J. Am. Chem. Soc.* **1995**, *117*, 5179–5197.
- [38] S. Mohan, L. Sim, D. R. Rose, B. M. Pinto, *Bioorg. Med. Chem.* **2010**, *18*, 7794–7798.
- [39] S. Mohan, K. Jayakanthan, R. Nasi, D. A. Kuntz, D. R. Rose, B. M. Pinto, *Org. Lett.* **2010**, *12*, 1088–1091.
- [40] a) S. M. Woodley, R. Catlow, *Nat. Mater.* **2008**, *7*, 937–946; b) A. R. Oganov, C. W. Glass, *J. Chem. Phys.* **2006**, *124*, 8–13; c) K. Sanderson, *Nature* **2007**, *450*, 771.
- [41] a) P. V. Groth, *Chemische Kristallographie*, vol. 1–5, Verlag Wilhelm Engelmann, Leipzig, **1906–1919**; b) L. Pauling, *J. Am. Chem. Soc.* **1929**, *51*, 1010–1026.
- [42] a) G. M. Day, T. G. Cooper, A. J. Cruz-Cabeza, K. E. Hejczyk, H. L. Ammon, S. X. M. Boerrigter, J. S. Tan, R. G. Della Valle, E. Venuti, J. Jose, S. R. Gadre, G. R. Desiraju, T. S. Thakur, B. P. van Eijck, J. C. Facelli, V. E. Bazterra, M. B. Ferraro, D. W. M. Hofmann, M. A. Neumann, F. J. J. Leusen, J. Kendrick, S. L. Price, A. J. Misquitta, P. G. Karamertzanis, G. W. A. Welch, H. A. Scheraga, Y. A. Arnautova, M. U. Schmidt, J. van de Streek, A. K. Wolf, B. Schweizer, *Acta Crystallogr., Sect. B* **2009**, *65*, 107–125; b) M. A. Neumann, F. J. J. Leusen, J. Kendrick, *Angew. Chem.* **2008**, *120*, 2461; *Angew. Chem. Int. Ed.* **2008**, *47*, 2427–2430.
- [43] a) D. J. Watkin, *Crystallogr. Rev.* **2010**, *16*, 197–230; b) G. M. Day, *Crystallogr. Rev.* **2011**, *17*, 3–52.
- [44] J. Bernstein, *Polymorphism in Molecular Crystals*, Oxford University Press, **2002**.
- [45] W. H. Baur, D. Kassner, *Acta Crystallogr., Sect. B* **1992**, *48*, 356–369.
- [46] A. I. Kitajgorodskij, *Molecular Crystals and Molecules*, Academic Press, New York, **1973**.
- [47] a) D. Cremer, J. A. Pople, *J. Am. Chem. Soc.* **1975**, *97*, 1354–1358; b) J. L. García Álvarez, G. A. Carriedo, M. E. Amato, G. M. Lombardo, F. Punzo, *Eur. J. Inorg. Chem.* **2010**, *28*, 4483–4491.
- [48] D. D. Perrin, W. L. F. Armarego, D. R. Perrin, *Purification of Laboratory Chemicals*, 2<sup>nd</sup> ed., Pergamon Press, Oxford, **1980**.
- [49] For a description of automated docking using a Lamarckian genetic algorithm and an empirical binding free energy function, see: G. M. Morris, D. S. Goodsell, R. S. Halliday, R.

- Huey, W. E. Hart, R. K. Belew, A. J. Olson, *J. Comput. Chem.* **1998**, *19*, 1639–1662.
- [50] M. F. Sanner, *J. Mol. Graphics Modell* **1999**, *17*, 57–61.
- [51] *MS Modeling Getting Started*, Accelrys Inc., San Diego, USA, **2003**.
- [52] A. D. Becke, *Phys. Rev. A* **1988**, *38*, 3098–3100.
- [53] C. Lee, W. Yang, R. G. Parr, *Phys. Rev. B* **1988**, *37*, 785–789.
- [54] H. Sun, *J. Phys. Chem. B* **1998**, *102*, 7338–7364.
- [55] a) M. B. Plazzer, D. J. Henry, G. Yiapanis, I. Yarovsky, *J. Phys. Chem. B* **2011**, *115*, 3964–3971; b) S. W. Bunte, H. Sun, *J. Phys. Chem. B* **2000**, *104*, 2477–2489; c) Z. Lifeng, L. Lianchi, H. Sun, *J. Phys. Chem. C* **2007**, *111*, 10610–10617; d) M. J. McQuaid, H. Sun, D. Rigby, *J. Comput. Chem.* **2004**, *25*, 61–71.

Received: June 8, 2011  
Published Online: October 26, 2011